

	MAPP ATBD	cloud microphysical properties
--	----------------------	---

Title: **ATBD cloud microphysical properties**

Doc. no: MAPP-ATBD-CMP

Issue: 1

Revision: 0

Date: 08. March 2000

	cloud microphysical properties ATBD	Doc. ID : MAPP-ATBD-CMP Name : Lothar Schüller Issue : 1 Rev.:0 Date : 08.03.2000 Page : ii
--	--	--

internal Distribution

Name

Quantity

external Distribution

Name

Quantity


Change Record

<u>Issue</u>	<u>Revision</u>	<u>Date</u>	<u>Description</u>	<u>Change pages</u>
1	0	8.3.2000	initial issue	

	cloud microphysical properties ATBD	Doc. ID : MAPP-ATBD-CMP Name : Lothar Schüller Issue : 1 Rev.:0 Date : 08.03.2000 Page : iii
--	--	--

Table of Contents

1.	INTRODUCTION.....	1
1.1	ALGORITHM IDENTIFICATION.....	1
2.	ALGORITHM OVERVIEW.....	1
3.	ALGORITHM DESCRIPTION.....	2
3.1	THEORETICAL DESCRIPTION	2
3.1.1	<i>Physics of the Problem</i>	2
3.1.2	<i>Mathematical Description of the Algorithm</i>	5
3.2	PRACTICAL CONSIDERATIONS	7
3.2.1	<i>Numerical computation considerations</i>	8
3.2.2	<i>Calibration and Validation</i>	8
3.2.3	<i>Quality Control and Diagnostics</i>	9
3.2.4	<i>Exception Handling</i>	9
3.2.5	<i>Output Product</i>	9
4.	ERROR BUDGET ESTIMATES.....	9
5.	ASSUMPTIONS AND LIMITATIONS	11
6.	REFERENCES.....	11
7.	MAPP DATA PRODUCT SUMMARY SHEET.....	11

 <p>Institut für Weltraumwissenschaften</p>	<h1>MAPP CMP</h1>	Doc : MAPP-ATBD-CMP Name : Lothar Schüller Issue : 1 Rev : 0 Date : 8.3.2000 Page : 1
--	-----------------------	---

1. INTRODUCTION

One major cloud effect on climate is the reflection of solar energy into space, which is not available for the absorption at earth surface. The amount of reflected radiation depends strongly on microphysical properties, mainly the cloud droplet size and cloud droplet concentration. Both parameter are related to aerosol-cloud interaction in the cloud development process. An increase in concentration of cloud condensation nuclei (CCN) due to natural and anthropogenic sources can enhance cloud albedo by an increase in droplet concentration and a reduction in droplet size.

In this document an algorithm is described to derive simultaneously droplet concentration and the effective particle radius of single layer stratocumulus and stratus clouds from measurements in the visible and near infrared. Basis of the algorithm is a new type of radiative transfer simulations taking into account the vertical structure of cloud parameter instead of simulate vertically homogeneous clouds. Artificial neural networks are used to invert the simulation results.

1.1 Algorithm Identification

cloud microphysical properties: droplet effective radius and droplet concentration

2. ALGORITHM OVERVIEW

The short-wave radiative properties of vertically homogeneous clouds are almost exclusively a function of optical thickness and droplet size distribution (Figure 1), that can be represented by an effective radius:

$$r_e = \frac{\int r^3 n(r) dr}{\int r^2 n(r) dr}$$

Currently, optical thickness and effective radius are used to parameterise the radiative transfer in general circulation models GCM (Slingo, 1989) and at the same time, these two parameters play an important role in the indirect effect of aerosols on climate. Measurements of the reflected solar radiation in the visible and near infrared can be used to derive δ_c and r_e , since the reflection in non absorbing window channels are primarily a function of the optical thickness and the radiation in the liquid water absorption bands (e.g. at 1.6 μm and 2.2 μm) are sensitive to the droplet size (Nakajima and King, 1990; Arking and Childs, 1985).

Operational algorithms has been developed based on the measurements in two channels, such as the effective radius retrieval algorithms for the Moderate Resolution Imaging Spectrometer MODIS (Nakajima and King, 1990) and the Advanced Very High Resolution Radiometer (AVHRR) (Wetzel and Vonder Haar, 1991). For optically thin clouds, these kind of retrievals lead to ambiguous results, i.e. the same combination of δ_c and r_e will result in the same combination of the two reflectances. To avoid these problems, an algorithm for the Along Track Scanning Radiometer (ATSR) has been developed that uses additional information which raises from the dual-look option of that instrument (Evans and Haigh, 1995). The approach described in this document will use additional spectral information to tackle the ambiguity problem.

Artificial neural network training is used to perform the inversion of radiative transfer simulations. The advantage of this method is that it can easily adopted to the complexity of the system and the processes, that are involved in the retrieval.

The microphysical characteristics of clouds can hardly described with a remotely sensed effective radius, because for almost all cloud types, the droplet size has an explicit vertical variability, whereas the remote sensed value is only sensitive to the microphysical properties of the upmost cloud layer. In contrast, droplet number concentration is often a height independent property, especially for stratocumulus clouds. A new conceptual model of the interaction of cloud microphysics and radiation, that includes the vertical inhomogeneity has been

developed, in order to be able to invert the radiative transfer in terms of cloud droplet concentration. The droplet concentration algorithm is based measurements within the same spectral channels and uses the same neural network inversion method.

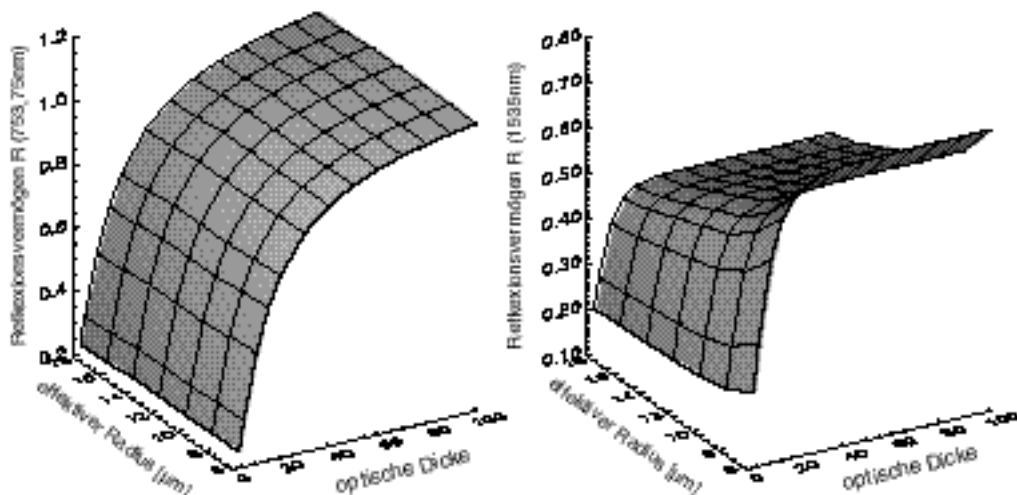


Figure 1: Dependence of reflectivity on the optical thickness and effective radius at two wavelength: 754nm (left) and 1535nm (right). Radiative transfer calculations has been performed with the MOMO code and is based on vertically homogeneous cloud layers.

3. ALGORITHM DESCRIPTION

3.1 Theoretical Description

3.1.1 Physics of the Problem

Figure 1 shows the reflectivity in a shortwave window channel and in a liquid water absorption channel in the near infrared as a function of optical thickness and effective radius. The calculations has been performed using the Matrix Operator Model (MOMO) of the FU-Berlin (Fischer and Graßl, 1991) and are based on vertical homogeneous cloud layers. This dependancy vary with solar zenith angle and viewing zenith angle. The influence of surface albedo can be strong especially for thin clouds and high surface reflectivity. The algorithm development and the application must therefore account for these effects. The illumination and observation geometry is well know for each pixel to be analysed. This knowledge can be used as auxillary data for the algorithms input. The surface albedo has to be estimated, either from surface property data bases such as the ISLSCP or from previous satellite overpasses over the same region. The estimated value will be used as algorithm input as well.

The most important source of error will be the microphysical and geometrical structure of the cloud. They cannot be estimated a priori, but have to be accounted for in the retrieval development. The radiative transfer simulations, that will be inverted by means of neural network training (see below) has to reflect the natural variability of the microphysical and geometrical parameters, that might influence the retrieval results. In a stratocumulus cloud, we usually find a strong dependancy of the effective radius with height above cloud base. This reflect the dynamical and thermodynamical processes during cloud development. Since the solar radiation penetrates mostly just the upper part of the cloud, we have to assign the remotely sensed cloud effective radius value to its real value at cloud top.

This principle restriction is unsatisfactory for studies (i.e. on the indirect effect of aerosols on climate, the Twomey effect) that address the microphysical structure of the whole cloud layer.

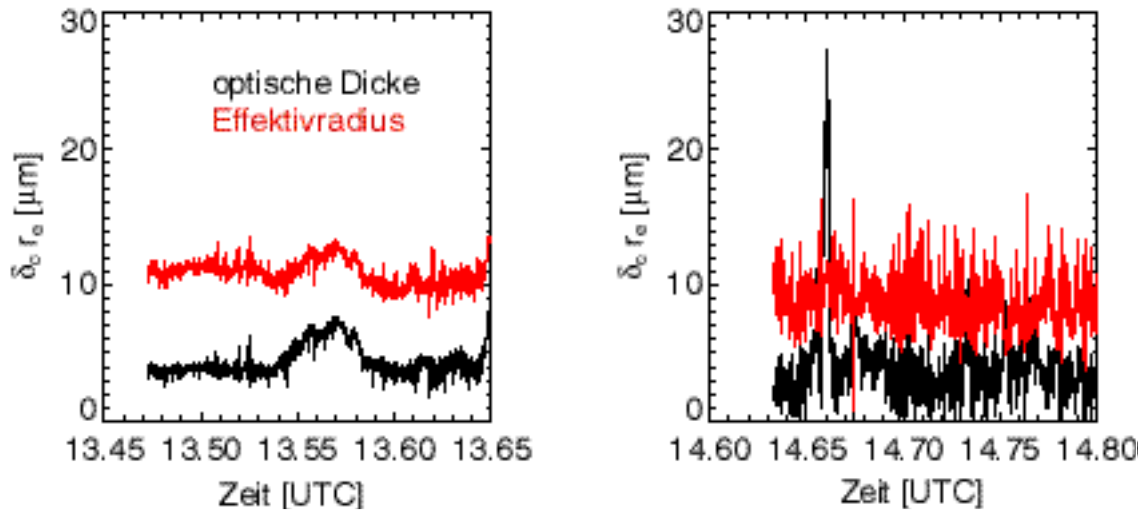


Figure 2: remotely sensed optical thickness and effective radius of a stratocumulus cloud layer. Reflectance measurements have been performed with an airborne spectrometer during the ACE-2 CLOUDYCOLUMN experiment. Left figure shows the result of 26th June 1997, right figure results of 9th July 1997.

Figure 2 is an example of retrieved cloud optical thickness and cloud effective radius. The radiation measurements have been performed with the airborne spectrometer OVID (Schüller et al., 1997) during the ACE-2 CLOUDYCOLUMN experiment 1997. Both retrieved quantities are obviously not independent from each other. They are highly correlated for all the flight leg of the campaign. This is a prominent problem that appears in studies with airborne and satellite remotely sensed data. Retrieved cloud optical and microphysical parameters from satellite measurements are not always consistent with the aerosol effect and with the prediction of theoretical models, e.g. a ISCCP dataset analysis shows, that cloud albedo and effective radius are positively correlated for optically thin clouds over ocean. This is in contradiction to the known fact, that especially this cloud type is the most susceptible one to the Twomey effect. The first analysis of OVID derived optical thickness and effective radius confirmed the presumption, that these parameters are not sufficient to observe changes of cloud properties due to pollution. The reason for these difficulties is the use of a vertically

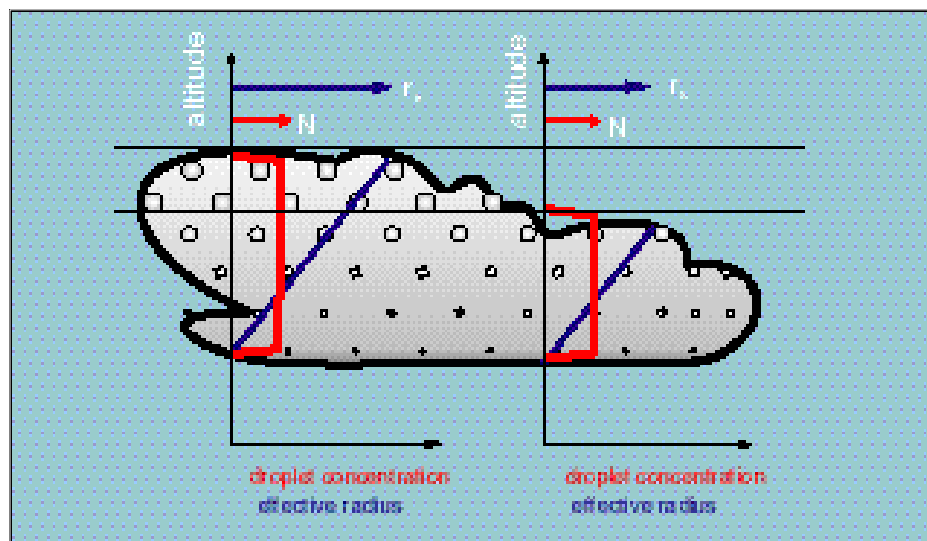


Figure 3: Effect of geometrical thickness variation on the remotely sensed effective radius

homogeneous plan-parallel radiative transfer model, which does not include the stratification of cloud microphysical properties. The retrieved values are positively correlated, because the reflected radiation, measured from above the clouds, carries information of the top-most layer of the cloud only. The droplet size at cloud top is dependent on the cloud depth (and thus on cloud optical thickness), which was clearly demonstrated by accompanied in situ measurements. The cloud top value of the droplet size can either be due to variations of the cloud geometrical thickness H or due to aerosol modified cloud microphysics (Figure 4). To separate these two effects, we implemented the adiabatic cloud profiles of effective radius and optical thickness into the radiative transfer simulations. The adiabatic assumption provides a possibility to link the cloud top droplet concentration $n_c(H)$ to the droplet number concentration N , which is almost constant through the cloud layer and is directly related to changes in CCN.

An important difference is, that the simulated cloud is not defined with the parameters δ_c and r_e , but with N and H . In the radiative transfer model the cloud layer is divided in a number of homogeneous sublayers. The values for δ_c and r_e are given for each layer by the adiabatic formulas.

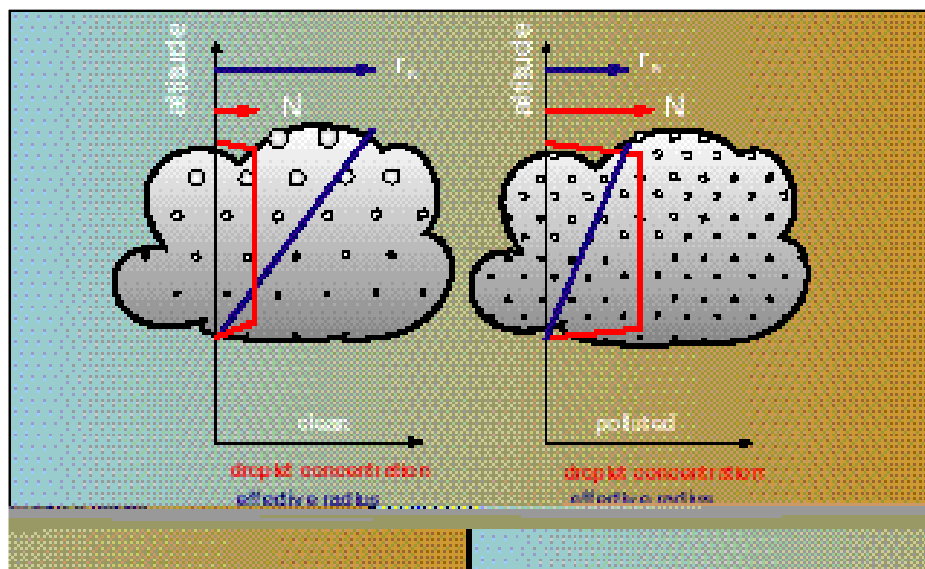


Figure 4: Effect of pollution on the remotely sensed effective radius (Twomey effect)

Figure 5 demonstrates clearly that the new representation is more suited to describe and observe the aerosol - cloud - radiation interaction processes. Two flight legs (60km) flown above horizontally homogeneous stratocumulus has been analysed to investigate the influence of polluted air masses on cloud reflectivity. The superimposed grids display the radiative transfer simulation results with the vertically homogeneous model, represented by isolines in δ_c and r_e (a and b), and with the vertically stratified model represented by isolines in N and H (c and d). Comparing measured and simulated reflectivities show that nearly the entire variation in measured reflectivity within one flight leg is due to variations in the cloud geometrical thickness H , the droplet concentration and thus the pollution level is almost constant. Although the averaged vertical extend of the cloud layer and the liquid water content was nearly the same on both days, the polluted clouds have a significant higher reflectance than the stratocumulus in the clean case. The data points are located along the isoline of $N=25\text{cm}^{-3}$ for the clean and $N=100\text{cm}^{-3}$ for the polluted case. These results establish a causal link between cloud droplet concentration as influenced by the amount of CCN and cloud reflectivity and are therefore an experimental evidence of the Twomey effect. The new parameterisation scheme and the validation with in situ measurements is described in more detail in the paper written by Brenguier et al., 2000.

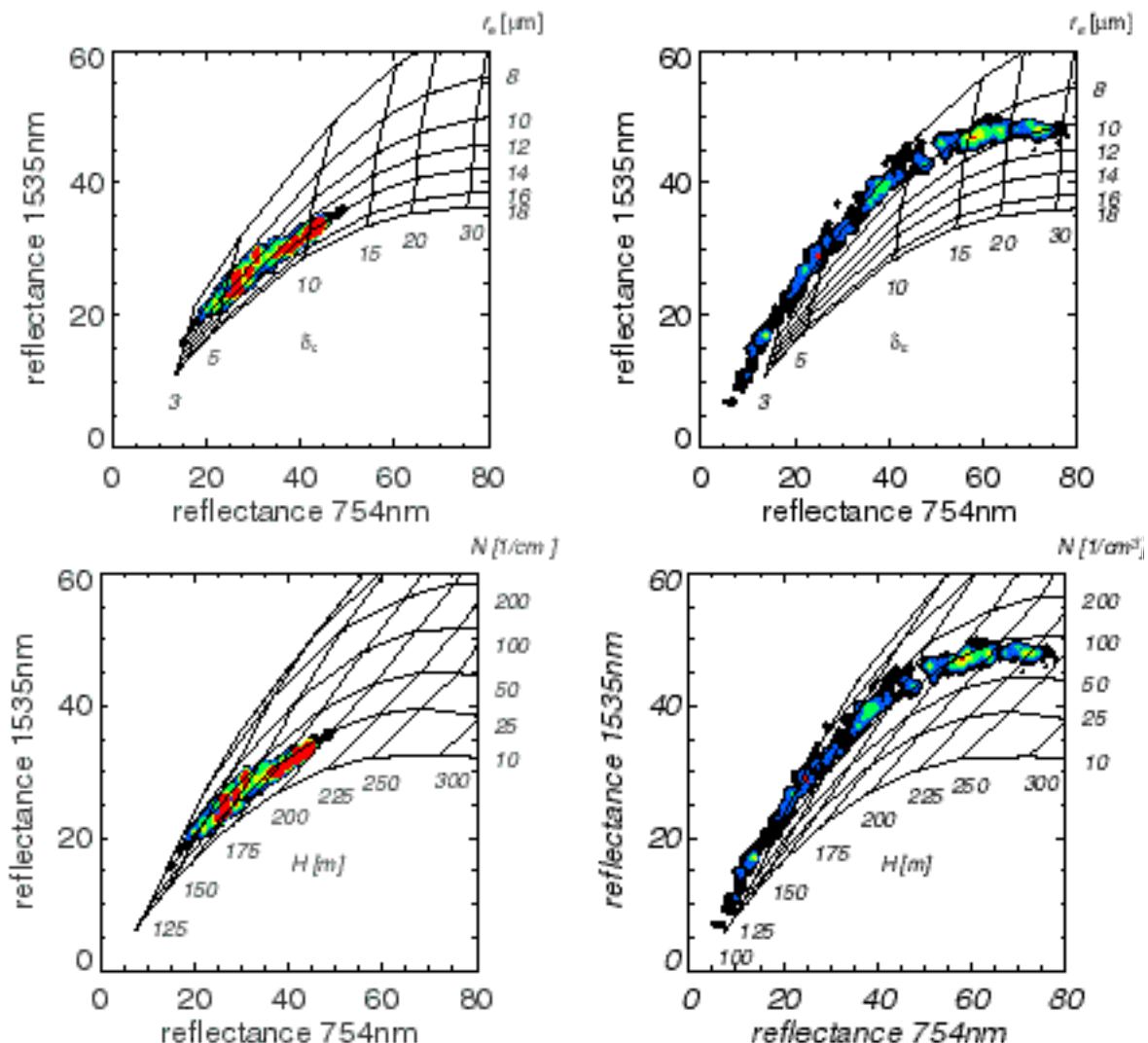


Figure 4: Two-dimensional histograms of reflectance measurements in the visible (754nm) and near infrared (1535nm). Radiative transfer simulation results are superimposed as isolines of effective radius and optical thickness (a and b) and isolines with cloud geometrical thickness and droplet concentration (c and d). Simulations have been performed for vertically homogeneous clouds. Left: reflectance data measured above stratocumulus clouds at June, 26th 1997 under clean air condition. Right: Reflectance data measured above stratocumulus clouds at July, 9th 1997 under polluted air condition.

3.1.2 Mathematical Description of the Algorithm

Radiative transfer calculation has been performed with the MOMO code to obtain radiance and reflectance values for the wavelength to be used in the retrieval (Schüller, 1999). The calculation will be adapted to the specific channel characteristics of the satellite sensors that will be used for the algorithms described in this document. The simulations have to cover a wide range of influencing parameters, either to be considered directly as input values or inherently in determine the variability of the inversion data base.

For the cloud droplet effective radius retrieval, the vertically homogeneous clouds are simulated with various cloud top heights, cloud depth, surface albedo, effective radius and cloud optical thickness. The variation of aerosol properties is also included in the inversion data base development.

The droplet concentration algorithm need simulations of vertically stratified clouds. The cloud layer is subdivided into a number of small sublayers, each assigned with a specific value of optical thickness (of the sublayer) and a

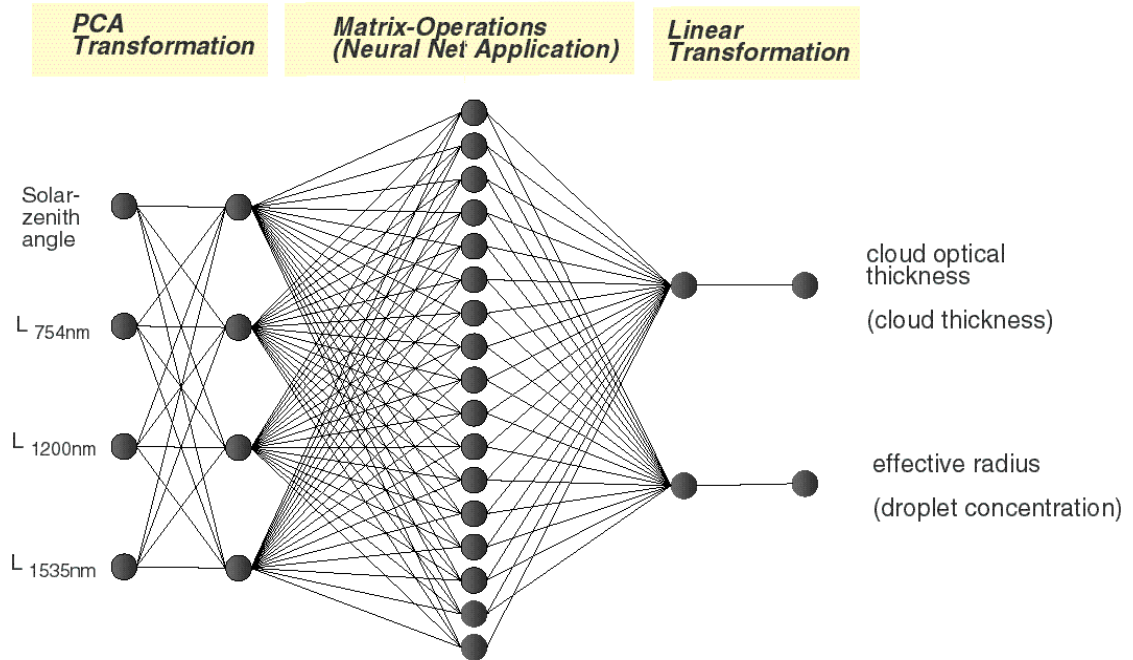


Figure 6: Structure of artificial neural network for the retrieval of cloud droplet effective radius and cloud droplet concentration

effective radius. These values are directly computed using the adiabatic formulas that describe the vertical profiles as a function of cloud droplet concentration and cloud depth. The forward problem, which is solved by radiative transfer simulations, can be displayed as:

$$\begin{pmatrix} \mathbf{q}_s \\ \mathbf{q}_v \\ \mathbf{d}_c \\ r_e \\ z_0 \\ z_{top} \\ \mathbf{a}_{surf} \end{pmatrix} \rightarrow \begin{pmatrix} L_1 \\ L_2 \\ L_3 \end{pmatrix} \quad \text{or} \quad \begin{pmatrix} \mathbf{q}_s \\ \mathbf{q}_v \\ N \\ H \\ z_0 \\ z_{top} \\ \mathbf{a}_{surf} \end{pmatrix} \rightarrow \begin{pmatrix} L_1 \\ L_2 \\ L_3 \end{pmatrix} \text{ respectively.}$$

From the simulation data base, learning patterns can be extracted where learning pattern means a pair of concrete vectors in the above shown relation. In order to find the invers relation:

$$\begin{pmatrix} L_1 \\ L_2 \\ L_3 \end{pmatrix} \rightarrow \begin{pmatrix} \mathbf{q}_s \\ \mathbf{q}_v \\ \mathbf{d}_c \\ r_e \\ z_0 \\ z_{top} \\ \mathbf{a}_{surf} \end{pmatrix} \quad \text{or} \quad \begin{pmatrix} L_1 \\ L_2 \\ L_3 \end{pmatrix} \rightarrow \begin{pmatrix} \mathbf{q}_s \\ \mathbf{q}_v \\ N \\ H \\ z_0 \\ z_{top} \\ \mathbf{a}_{surf} \end{pmatrix} \quad \text{respectively,}$$

artificial neural network training will be applied. The (simplified) structure of a neural network is shown in Figure 6. It consists of input and output vectors as well as an hidden layer vector, where each element represents a neuron. The connections between the neuron are assigned to weights, carrying signals. The neurons of the hidden and output layer transforming incoming signals according to an activation function of the form:

$$\mathbf{s}_i(x) = \frac{1}{1 + e^{-tx}}$$

All connections from neurons of layer n to layer n+1 can be represented by a matrice of weights W_n where each element $W_{i,j}$ is the weight of the connection from neuron i of layer n to neuron j of layer n+1. The data processing of a three-layer network can be expressed as:

$$\text{Output} = \mathbf{s}(W_2 \times \mathbf{s}(W_1 \times \text{Input})).$$

This is a combination of linear (matrix multiplication) and non-linear (activation function) transformations. The two other layers of Figure 6 represents a pre- and postprocessing of the vectors. A principal component analysis performs a de-correlation of the input vectors and a linear transformation scales input and output vectors to be within the interval [0,1]. These processeings accelerates the finding of the optimal weights. The backpropagation learning process searches the weights, that minimize the error of the retrieval function. After Rumelhard and McClelland, 1986, this involves five steps:


1. Initialisation of the matrices with random numbers
2. Processing of one or more learning patterns with the neural net
3. Calculation of the difference of net output and original value of the learning pattern
4. Determination of the gradient matrice, $G_n(i,j)$ of the error function by backpropagation of the error signals through the network
5. Correction of weights according to the calculated gradients:

$$W_n^{i,j} = W_n^{i,j} + G_n^{i,j}$$

Steps 2 to 5 will be repeated until the neural net is able to represent a number a test patterns with sufficient accuracy.

3.2 Practical Considerations

The calculated weight matrices define a neural network, that can process real remote sensing data (sensor images and auxillary data) to derive geophysical parameters, such as effective radius and droplet concentration. The algorithm itself is quite small and fast, since the code just have to include the above mentioned processing equation and the weights of the network. The matrices of the effective radius retrieval e.g. are stored in a file of 1.8 kByte size. Careful attention is required during the application to read data. The training of neural nets is completely a statistical approach with no physical model behind. Application outside the range of the training data could therefore lead to unphysical results and has to be avoided. On the other hand, this is also the reason to be very careful with the selection of the training data set (learning patterns). They should represents the range, but also the statistics of the variation of all physical parameters, that have influence on the retrieval.

 Institut für Weltraumwissenschaften	MAPP CMP	Doc : MAPP-ATBD-CMP Name : Lothar Schüller Issue : 1 Rev : 0 Date : 8.3.2000 Page : 8
--	-------------------------------	---

3.2.1 Numerical computation considerations

TBD

3.2.2 Calibration and Validation

Three possible strategies for calibration and validation will be suggested here, that are based on statistical (satellite intercomparison), experimental (airborne measurements) and theoretical (simulations) methods.

The main difficulty in building a reference data base for cloud optical and microphysical properties is the large variability of the microphysical field and the fact that microphysical properties are not linearly related to the optical properties in a heterogeneous cloud layer. Scaling effects are thus critical between the very small scale of the in situ measurements (less than a meter) and the satellite observations (up to 1 km). The validation of the satellite measurements can be achieved in three steps.

3.2.2.1 Satellite intercomparison.

Data from different satellite sensors, e.g. AVHRR, MERIS, SEVIRI, AATSR and MODIS images can be selected for collocation in space and time, with a priority on images taken during field experiments. Cloud parameters will be retrieved and compared. This methodology will provide an estimate of the uncertainty based on the variability of the results from the various retrieval techniques.

3.2.2.2 Plane parallel validation with close remote sensing.

The most accurate validation can be achieved by field experiments with extensive use of sophisticated instrumentation and platforms. The instrumental setup should consist of airborne remote sensing instruments, that can simulate satellite measurements but with higher spatial resolution and better accuracy (calibration) and in situ sensors to directly measure the microphysical properties from an in cloud flying aircraft. Additional instrumentation can be very useful for a detailed characterisation of second order influencing parameters (e.g. aerosol and surface properties).

The methodology includes the validation of the close remote sensing measurements (application of the satellite algorithms to data from airborne spectrometer) at the scale of the same cloud cells observed by in situ measurements of droplet size and droplet concentration. The close synchronization and collocation of the remote sensing aircraft (RSA) and the in situ aircraft (ISA) tracks are crucial in this phase. Cloud cells can be identified and selected in both data sets for comparison between values of effective radius and droplet concentration measured in situ and the values retrieved from remote sensing. Radiative transfer calculations will then be performed with a stratified plane parallel model of cloud initialized with the in situ measured values of droplet number concentration, cloud base and top altitudes, and a theoretical profile of liquid water content. The calculation provides reference values at the top of the convective cells, which are used to validate the retrieved values at the same location. The optical properties will then be extrapolated to the scale of the satellite pixel by averaging over the 2-D fields of optical thickness from imaging spectrometer on board the RSA. This procedure provides a validation of the satellites estimates within the limit of the plane parallel hypothesis, that is the hypothesis of horizontal uniformity of the cloud microphysical fields in radiative transfer calculations with the matrix operator model.

3.2.2.3 Heterogeneous cloud numerical validation.

Three dimensional effects can disturb efficiently the retrieval of cloud parameters, that are derived using simulations under plan-parallel assumption. The influence of these effects can be investigated by means of Monte Carlo radiative transfer models, that can be applied to clouds, produced with dynamical models such as Large Scale Eddy simulations (LES).

The heterogeneity of the cloud microphysical fields cannot be simply simulated with a random generator because it is not isotropic but rather governed by the convective activity and the large scale structures of the turbulence in the boundary layer. Only a physically based large eddy simulation model is able to realistically reproduce such structures, together with the mean vertical profile of liquid water content in stratocumulus. The LES model shall solve explicitly scales at which the structures are not isotropic, while subgrid parameterisations are used for isotropic turbulence at smaller scales. The model will thus be run in two steps with a first horizontal domain of 50 km square at a resolution of 100 m, with bulk microphysics and secondly

in a nested horizontal domain of 1 km (satellite pixel scale) with a resolution of 10 m and less, and subgrid parameterizations of the microphysics.

The model will be constrained to statistics of cloud dynamical structure as measured e.g with Radar or Lidar, by tuning the initialisation modes of turbulence and the subgrid parameterization. The same procedure will be repeated for a set of typical cases, in terms of cloud geometrical thickness and droplet number concentration. The simulations, with structural properties validated by the measurements, will then be used with the Monte Carlo model of radiative transfer to precisely estimate the heterogeneous bias and get the best possible reference of cloud optical properties for the validation of the satellite products.

3.2.3 Quality Control and Diagnostics

TBD

3.2.4 Exception Handling

The entity of learning patterns in the training data base of the neural network training limits the applicability of the resulting algorithms. Calculation of geophysical parameters is not allowed, if any of the input parameters exceed the range of variation in the training file. The valid range information will be made available to the processor either as an external auxiliary file or internally within the specific retrieval modul. For pixels with invalid input range further processing will be suppressed and an error flag will be raised.

For the droplet concentration algorithms further restriction apply concerning cloud type (see section 5: Assumptions and limitations), which will be tackled by an additional flag.

3.2.5 Output Product

cloud droplet effective radius

cloud droplet concentration

4. ERROR BUDGET ESTIMATES

For the cloud droplet effective radius retrieval, the differences between the two-channel and the three-channel approach has been analysed comparing the absolute deviations of the retrieved effective radius and the true (simulated) value as well the sensitivity to instrumental noise. In Figure 7 this comparison is shown scatter plots for different noise levels for both types of algorithms.

Although the overestimation of r_e is appears in the three channel procedure, the absolute deviation is reduced significantly compared the the two-channel algorithm.

Table 1 is the summary of a noise sensitivity test with simulated radiances. Mean deviation and variance are shown as a function of simulated sensor noise.

Table 1: Results of an error and sensitivity analysis. Dependence of mean deviation and variance on instrumental noise as well as on number of channels used for the retrieval. The analysis is bases on 900 cases for optical thickness between 5 and 99 and effective radius between 0 and 15 μ m.

noise		0%	1%	4%	10%	30%
2 channel	mean deviation	0.21038	0.21563	0.27026	0.5159	-0.11263
	variance	2.82240	2.81208	2.89420	3.79503	7.31836
3 channel	mean deviation	-0.06219	-0.03378	-0.03378	-0.17791	-3.65859
	variance	1.73991	1.71311	2.87674	5.764476	8.8779

Titel:

Erstellt von:
 GNU Ghostscript 510 (epswrite)
 Vorschau:
 Diese EPS-Grafik wurde nicht gespeichert
 mit einer enthaltenen Vorschau.
 Kommentar:
 Diese EPS-Grafik wird an einen
 PostScript-Drucker gedruckt, aber nicht
 an andere Druckertypen.


Titel:

Erstellt von:
 GNU Ghostscript 510 (epswrite)
 Vorschau:
 Diese EPS-Grafik wurde nicht gespeichert
 mit einer enthaltenen Vorschau.
 Kommentar:
 Diese EPS-Grafik wird an einen
 PostScript-Drucker gedruckt, aber nicht
 an andere Druckertypen.

Titel:

Erstellt von:
 GNU Ghostscript 510 (epswrite)
 Vorschau:
 Diese EPS-Grafik wurde nicht gespeichert
 mit einer enthaltenen Vorschau.
 Kommentar:
 Diese EPS-Grafik wird an einen
 PostScript-Drucker gedruckt, aber nicht
 an andere Druckertypen.

Figure 7: Scatter diagram of simulated and retrieved effective radii determined by a two channel version (left) and a three channel version (right). An artificial noise has been introduced to the simulated radiances before algorithm application. Noise 0% (upper graphs), 1% (middle graphs) and 10% (lower graphs).

 Institut für Weltraumwissenschaften	MAPP CMP	Doc : MAPP-ATBD-CMP Name : Lothar Schüller Issue : 1 Rev : 0 Date : 8.3.2000 Page : 11
--	-------------------------------	--

5. ASSUMPTIONS AND LIMITATIONS

For the retrieval of effective radius and droplet concentration, reflectances within a short-wave window channel and within a channel in a near infrared liquid water absorption band. Additional spectral information can be used to increase accuracy and applicability but is not necessarily required. The ENVISAT platform provides with the AATSR these requirements., but also MODIS, AVHRR, MOS and GLI data can be processed with such kind of retrieval procedure.

The droplet concentration retrieval is restricted to boundary layer stratocumulus cloud types, since the underlying adiabatic model is valid only for this cloud type. A cloud classification is therefore required, before the algorithm can be applied. Cloud top height information is very useful for such the discrimination. The MERIS cloud top pressure product is particularly suited to classify AATSR images. The spectral specification of MOS and GLI allow the simultaneous retrieval of cloud top height (with oxygen-A band) and droplet concentration (liquid water absorption band). The adiabatic assumption, that is inherently applied in the droplet concentration algorithm reflects situation with the maximum amount of condensed water. This strong prerequisite is not fulfilled for most of the pixels, even if they are clearly identified as stratocumulus clouds. This leads to a large uncertainty of the retrieval, however, as has been validated with data from the CLOUDCOLUMN experiment, the new remote sensing retrieval is able to detect changes in microphysical structure and to estimate the pollution level. At current status of the research and development, the cloud droplet concentration product is clearly more a qualitative product and a quantitative approach.

6. REFERENCES

Arking, A. and J. D. Childs, 1985, Retrieval of cloud cover parameters from multispectral satellite measurements, *J. Clim. Appl. Met.*, 24, 322-333.

Brenguier, J. L., H. Pawlowska, L. Schüller, R. Preusker, J. Fischer and Y. Fourquart, 2000: Radiative properties of boundary layer clouds: Effective radius versus droplet concentration. Accepted by *J. Atmos. Sci.*

Evans, S. J. and J. Haigh, 1995: The retrieval of optical depth and effective droplet radius of clouds from solar reflection measurements using Along Track Scanning Radiometer-2 (ATSR-2), *Geophys. Res. Lett.*, 22, 695-698.

Fischer, J. and H. Graßl: Detection of cloud-top height from backscattered radiances within the oxygen-A band. Part I: Theoretical study. *J. Appl. Met.*, 30, 1245-1259

Nakajima, T. and M. D. King, 1990: Determination of optical thickness and effective particle radius of clouds from reflected solar radiation measurements, Part I : Theory, *J. Atmos. Sci.*, 47, 1878-1893


Rumelhart, D. and J. McClelland, 1986: *Parallel Distributed Processing*, MIT press

Schüller, L., 1999 : *Fernerkundung von klimarelevanten Wolkeneigenschaften mit satelliten und flugzeuggestützten Radiometers, Strahlung in Atmosphäre und Ozean, Beiträge zur Fernerkundung*, Institut für Weltraumwissenschaften, Freie Universität Berlin.

Schüller, L., J. Fischer, W. Armbruster and B. Bartsch, 1997: Calibration of high resolution remote sensing instruments in the visible and near infrared, *Adv. Space Res.*, 19, 1325-1334.

Slingo, A., 1989: A GCM parameterisation of the short-wave radiative properties of water clouds, *J. Atmos. Sci.*, 46, 1419-1427

Twomey, S. 1977: The influence of pollution on the shortwave albedo of clouds, *J. Atmos. Sci.*, 34, 1149-1152

 Institut für Weltraumwissenschaften	MAPP CMP	Doc : MAPP-ATBD-CMP Name : Lothar Schüller Issue : 1 Rev : 0 Date : 8.3.2000 Page : 12
--	-------------------------------	--

Wetzel, M. A. and T. H. Vonder Haar, 1991: Theoretical development and sensitivity test of a stratus cloud droplet size retrieval method for AVHRR-K/L/M, Rem. Sens. Environ. 36, 105-119.

MAPP DATA PRODUCT SUMMARY SHEET

Product name:	
Product code:	
Product Level:	
Description of the Product:	
Product Parameters:	
Coverage	
Packaging:	
Units:	
Range:	
Sampling:	
Resolution:	
Accuracy:	
Geo-location:	
Format:	
Appended data:	
Frequency of generation:	
Size of product:	
Additional information:	
Identification of bands used in algorithm	
Assumption on MERIS input data	
Identification of ancillary and auxiliary data	
Assumptions on ancillary and auxiliary data	